Self-organization of multiple polariton-polariton scattering in semiconductor microcavities

D. N. Krizhanovskii,[1] S. S. Gavrilov,[2,3,4] A. P. D. Love,[1] D. Sanvitto,[1] N. A. Gippius,[3,4] S. G. Tikhodeev,[3,4]
V. D. Kulakovskii,[2] D. M. Whittaker,[1] M. S. Skolnick,[1] and J. S. Roberts[1]

[1]*Department of Physics and Astronomy, University of Sheffield, Sheffield S3 7RH, United Kingdom*

[2]*Institute of Solid State Physics, Russian Academy of Sciences, Moscow 142432, Russia*

[3]*A. M. Prokhorov General Physics Institute, Russian Academy of Sciences, Moscow 119991, Russia*

[4]*LASMEA, UMR 6602 CNRS, Université Blaise Pascal, 63177 Aubière, France*

Sharp transformations of polariton-polariton scattering patterns in a semiconductor microcavity with an increase in pump intensity are observed. These transformations are manifestations of nonequilibrium first-order phase transitions in a strongly driven multimode Bose system. The effect arises from the interplay between the bistability of the pumped polariton mode and the parametric instability in the nonlinear polariton system.

I. INTRODUCTION

There is worldwide interest in the study of polaritons in strongly coupled semiconductor microcavities (MCs).[1] Interesting nonlinear phenomena associated with exciton-exciton interactions may arise in such systems. In addition, quantum effects, such as squeezing and complementarity of idler polaritons, have been reported.[2,3] Recently, high-density macroscopically occupied polariton states, with properties expected for Bose–Einstein condensates, have been observed due to incoherent exciton-polariton relaxations in CdTe (Ref. 4) and GaAs (Ref. 5) MCs. Signal and idler states[6–8] formed from stimulated polariton-polariton pair scattering for resonant excitation into the lower polariton (LP) branch are also expected to exhibit properties similar to those of Bose–Einstein condensates even though the system is strongly nonequilibrium.[9]

In this paper, we show that the highly occupied MC polariton system exhibits a type of multimode threshold behavior, not previously observed, to the best of our knowledge, in the physics of nonlinear systems. This behavior is a result of the unique continuous transverse mode dispersion in MCs, which exhibits a point of inflection and has a finite energy at **k**=0. In our experiments, we employ cw resonant excitation, with the excitation significantly detuned to higher energies with respect to LP dispersion. At powers below threshold (P_{th}), the polaritons scatter to states in a figure 8 (Refs. 10 and 11) in k space, as determined by energy and momentum conservation. However, at $P \sim P_{th}$, we observe an abrupt transition of the scattering from these states with **k** ≠ 0 to one that is strongly localized at **k** ≈ 0. This state becomes macroscopically occupied and remains stable at higher excitation powers.

Analytical investigation of the instabilities of the solution of the Gross–Pitaevskii equations (for one macroscopically occupied pump mode) and numerical integration[12–15] show that the transition arises from the interplay of instabilities in the driven polariton system. In particular, since the pumped mode exhibits bistability (multistability if the polariton polarization state is taken into account[16]), the system is driven into a region of strong parametric instability, leading to a breakup into many "signal-idler" pairs over a large range of

k. It leads to the amplification of many unstable harmonics, as shown by numerical simulation. However, this state is unstable, and further system evolution takes the form of self-organization with the result that, eventually, only one macroscopically occupied signal-idler pair is amplified, i.e., a signal at **k** ∼ 0 and an idler at **k** ∼ 2$\mathbf{k}_p$ (where $\mathbf{k}_p$ is the in-plane pump momentum).

The observed transition corresponds to a type of behavior in nonequilibrium systems and can be described only within a multimode model, which takes into account macroscopic occupation of many polariton states, to which the scattering is permitted. An excellent agreement of the theory with the experimental observations is obtained. The existing three-mode optical parametric oscillator models for stimulated polariton-polariton scattering in MCs[10,17–21] cannot be used to explain the observed transition because (i) they cannot predict the final $\mathbf{k}_{s,i}$ that are selected by the system and (ii) they neglect other polariton modes that, as we will show, are very important in the self-organization process.

II. EXPERIMENT

The microcavity studied had a structure very similar to that of Ref. 6. Several regions of the MC were investigated, all with 6 meV Rabi splitting and approximately zero detuning between the exciton and cavity modes. The beam from a tunable laser was focused to a ∼30 μm diameter spot on the sample at an angle of incidence of $\vartheta \approx 11°$ corresponding to $k_x \approx 1.4$ μm^{-1}. Lower polariton photoluminescence was studied in a two-dimensional (2D) momentum space (k_x, k_y) at several detunings between the energy of the laser excitation and that of the LP dispersion.

A simplified schematic of the polariton-polariton parametric scattering at low pump intensity is illustrated in Fig. 1. The energy of the laser, i.e., $E_p \approx 1.4521$ meV, was significantly detuned (by ∼0.5 meV) with respect to the unperturbed LP branch at low power (see the circle in Fig. 1) and then fixed during the experiment. In the case of smaller (near zero) pump detuning, the signal and idler are expected to form a figure 8 around **k**=0 and 2$\mathbf{k}_p$ in a 2D wave vector space,[10,11,22] as shown by the dashed curve in Fig. 1(b). Self-stimulated polariton-polariton scattering to the states **k**=0
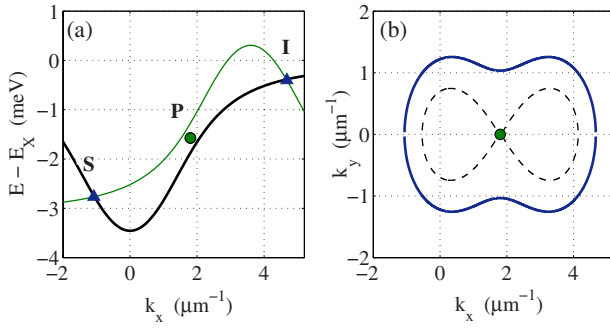
FIG. 1. (Color online) [(a) and (b)] Schematic of the polariton-polariton scattering in a MC at low excitation power. The thick and thin solid lines in (a) are $E_{LP}(\mathbf{k})$ (the LP branch) and $2E_p - E_{LP}(2\mathbf{k}_p - \mathbf{k})$, respectively, for $k_y = 0$. The circle and triangles labeled as P, S, and I show the (E, k_x) positions of the pump and the corresponding signal and idler. Dashed and solid 8-shaped figures in (b) show the scattered polaritons in the (k_x, k_y) plane for zero and positive [as shown by the circle in (a)] detunings between the pump and the LP branch, respectively.

and $2\mathbf{k}_p$ has been previously observed in Refs. [6–8]. With an increase in detuning $E_p - E_{LP} > 0$, the pattern is expected to transform into a distorted (expanded) figure 8, as shown by the solid curve in Fig. 1(b), with the left ("signal") part shifting further toward negative $k_x < 0$.

The intensities $[I(P)]$ and the linewidths [full width at half maximum (FWHM)] of polariton emission as a function of the excitation power P recorded at $\mathbf{k} = 0$ (circles) and $\mathbf{k} = (0, 0.7)$ μm^{-1} (squares) are presented in Figs. 2(a) and 2(b), respectively. The upper panels in Fig. 3 display the measured 2D distributions $I(\mathbf{k})$ of the LP emission in a wave vector space $\mathbf{k} = (k_x, k_y)$ at several excitation powers. The emission was integrated over the energy range (1.45–1.4519 eV) below the pump energy E_p. The bottom panels in Fig. 3 show the corresponding images in (E, k_y) space recorded at $k_x \approx 0$. The images in k space (top panels in Fig. 3) were obtained by sequentially measuring $I(k_y, E)$ for a grid of k_x with steps of 0.06 μm^{-1}.

At low power, $P = 1$ mW, the intensity distribution $I(\mathbf{k})$ is approximately homogeneous in (k_x, k_y) space [Fig. 3(a), top]; the distribution in (E, k_y) space shows the familiar LP dispersion [Fig. 3(a), bottom], which is nearly parabolic at small $\mathbf{k}$.

Simultaneously, as seen in Fig. 2(a), the dependences $I(P)$ at $\mathbf{k} = 0$ and $\mathbf{k} = (0, 0.7)$ μm^{-1} exhibit a linear increase with P at $P < 10$ mW. In this case, the relaxation of pump polaritons to lower energy states occurs due to interactions with acoustic phonons and weakly coupled localized excitons, resulting in a homogeneous polariton distribution. Nevertheless, at low power, the polariton distribution is not thermalized since the relaxation with phonons occurs on a time scale of ~ 20 ps, which is larger than the polariton lifetime (~ 5 ps).

At $P \sim 10$ mW, there is an onset of a new effective scattering channel, namely, direct spontaneous polariton-polariton scattering of two pump polaritons into ($k \neq 0$) signal and idler scattered polaritons. This mechanism becomes dominant at higher excitation powers and, as we will show below, determines the pattern of polariton emission. Because
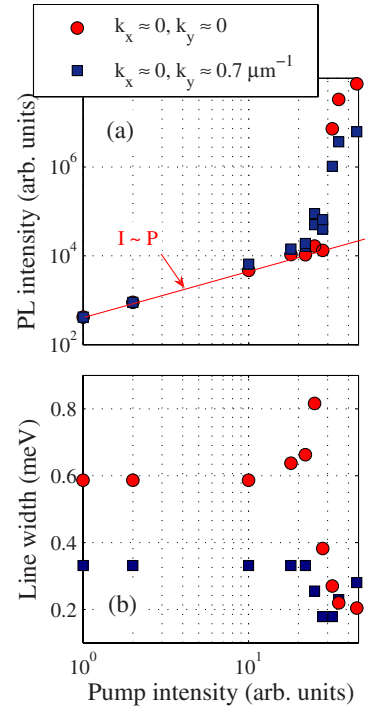

FIG. 2. (Color online) (a) The measured intensities and (b) energy linewidths of the signal at $k_x \approx 0$ and $k_y \approx 0$ (circles) or at $k_y \sim 0.7$ μm^{-1} (squares) as functions of the pump intensity.

of detuning, as explained above the formation of a distorted 8-shaped figure around $\mathbf{k} = 0$ and $2\mathbf{k}_p$ in a 2D wave vector space is expected.[10,11]

The onset of polariton-polariton scattering is supported by the observed transformation of the intensity distribution in k space at $P = 10$ mW [see Fig. 3(b), top]: A near-circular shape arises with intensity maxima at $|\mathbf{k}| \sim 0.5–0.7$ μm^{-1}. This corresponds to the left (signal) half of the 8 shape in Refs. [10] and [11]—we do not show the idler polaritons. As seen in Fig. 3(b) (bottom panel), the states with smaller $|\mathbf{k}|$ become more depleted with respect to those at higher energy and higher momentum states. Additional evidence for polariton-polariton scattering is that intensity $I(P)$ at $\mathbf{k} = (0, 0.7)$ μm^{-1} starts to superlinearly increase with power at $P > 10$ mW, whereas $I(P)$ recorded at $\mathbf{k} = 0$ remains nearly linear, as seen in Fig. 2(a).

At $P = 18$ mW, the intensity distribution $I(k_x = 0, k_y)$ acquires pronounced maxima at around ± 0.7 μm^{-1} [Fig. 3(c), bottom]. As seen from the corresponding distribution $I(\mathbf{k})$ [Fig. 3(c), top], there is a higher efficiency of polariton-polariton scattering to the states with k vectors close to that of the pump. This is because there are higher losses for the scattering from the pump to the excitonlike idlers at larger k vectors and higher energies and to the corresponding signals at negative k_x. The losses arise from additional scattering processes at idler states mainly due to inhomogeneous exciton broadening.[11]

With a further increase in excitation power, multiple LP-LP scattering reveals striking features that contradict the predictions of the standard four-wave mixing theory.[10,17,18] Figure 3(d) (top) shows that at $P = 28$ mW, $I(\mathbf{k})$ exhibits several strong maxima at around ± 0.7 μm^{-1}, and significant
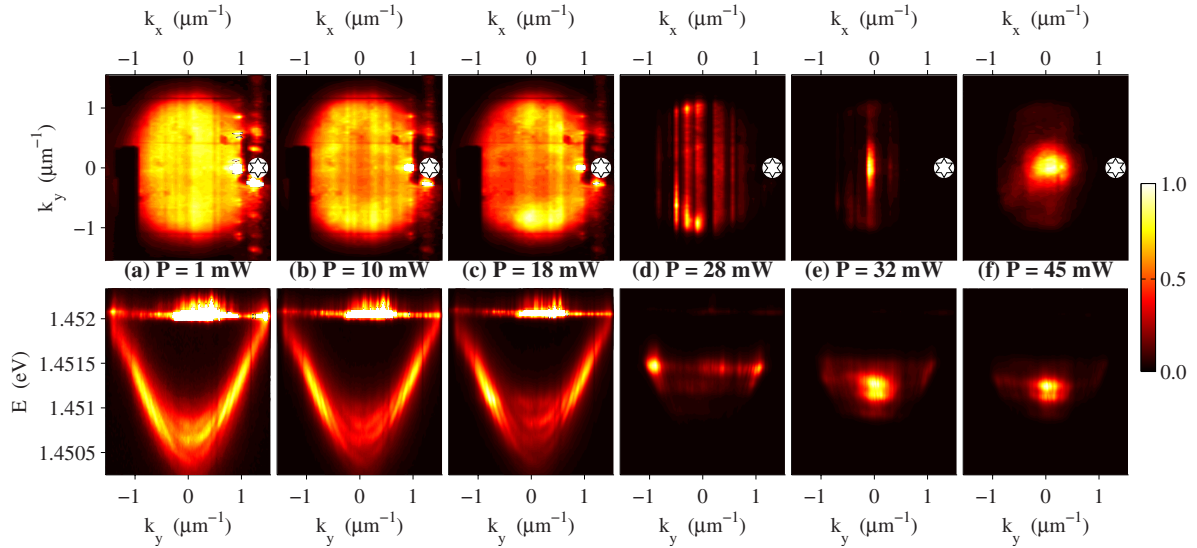
FIG. 3. (Color online) Measured lower polariton PL distributions as functions of wave vector k_y, k_x (top panels) and of energy and wave vector (E, k_y) (bottom panels) at different excitation intensities. The pump position $k_x = 1.4$ μm^{-1}, $k_y = 0$ is marked by a star in the top panels. Colors show the normalized PL intensity. Only the "signal" part of the scattered PL is shown, and the "idler" counterpart is omitted. The rectangular shadow seen on the left of top panels (a)–(c) is the metallic wire, which holds the mirror directing the excitation laser beam to the sample. The vertical line observed on the right of top panels (a)–(c) at $k_x = 1.4$ μm^{-1} is the scattered light of the exciting laser pump.

spectral narrowing (FWHM=0.17 meV) of the corresponding emission by a factor of 2 occurs [Figs. 2(b) and 3(d), bottom]. Also, its intensity starts to grow faster than P^2 at $P > 20$ mW, as shown in Fig. 2(a). Such observations indicate the increasing temporal coherence of the polariton emission due to final state stimulation. There is a weaker stripe-like polariton emission observed at k vectors between the maxima at ± 0.7 μm^{-1} [Fig. 3(d), top]. The origin of this emission is discussed in Sec. III.

With a further increase in P by 5%–10% above the threshold ($P_{\text{thr}} \approx 28$ mW), an abrupt transition of the stimulated process from $k_y \neq 0$ to one strongly centered at $\mathbf{k} \sim 0$ μm^{-1} is observed, as shown in Figs. 2(a) and 3(e). Above the threshold, the intensity of the stimulated emission at $k \sim 0$ is increased by 2 to 3 orders of magnitude with respect to that of the polariton emission below the threshold [Fig. 2(a)], and its linewidth is reduced from 0.6 to 0.2 meV [Fig. 2(b)]. Such emission remains stable at higher excitation powers [Fig. 3(f)]. The width (FWHM) of the localized mode in Figs. 3(e) and 3(f) is about $0.3-0.5$ μm^{-1} in k space. This value indicates a localization area of $10-15$ μm in real space, which was previously observed in Ref. 23 on similar samples.

We note that such an abrupt transition of the pattern of polariton-polariton scattering was not previously observed in Ref. 11, which was devoted to the case of spontaneous polariton-polariton scattering with a small occupation number of the final signal and idler states. By contrast, in our experiment, macroscopic occupation of the final signal and idler states is reached, which results in the phenomena observed. The observed behavior is in very good qualitative agreement with the analytical investigation of the instabilities and numerical integration of the Gross–Pitaevskii-type equations for the driven cavity-polariton dynamics[13–15] in a 2D wave vector space.

III. THEORETICAL ANALYSIS

In Refs. 13–15 the semiclassical Gross–Pitaevskii-type equations for the intracavity QW excitonic polarization $\mathcal{P}(\mathbf{k}, t)$ and electric field $\mathcal{E}_{\text{QW}}(\mathbf{k}, t)$ as functions of the external driving $\mathcal{E}_{\text{ext}}(\mathbf{k}, t) = \delta_{\mathbf{k}, \mathbf{k}_p} \mathcal{E}(t) \exp(-iE_p t)$ have been formulated. In this case, the polariton density at a given k vector is proportional to $|\mathcal{P}(\mathbf{k}, t)|^2$. To explain the experimental results, the stability of the solution for one macroscopically occupied (pumped) mode, as in the case of the experiment, was analyzed. The main results are summarized in Fig. 4.

In the case of a planar cavity, the resonant frequency for a given in-plane momentum depends on the intensity of the field inside the cavity and is blueshifted for larger intensities due to polariton-polariton interactions. As a result, the field inside the cavity exhibits a characteristic S-shape dependence as a function of pump intensity [Fig. 4(a)] with two points of discontinuity (squares). These points correspond to the high intensity boundary of the polariton bistability area (see also Refs. 19 and 20).

First, to analyze stability with respect to intermode scattering, we calculate the polariton decay rate Γ (imaginary part of the scattered polariton eigenenergy). For each scattered polariton mode $\mathbf{k}$, its amplitude is $|\mathcal{P}(\mathbf{k}, t)| \propto \exp[\Gamma(\mathbf{k})t]$, so that the polariton mode is amplified if Γ is positive. It is found that $\Gamma(\mathbf{k})$ is crucially dependent on the pumped mode amplitude; Figs. 4(b) and 4(c) show the distribution of $\Gamma(k_x, k_y)$, which is calculated at the two driven polariton densities shown by the squares in panel (a).

In the low-density regime, the decay rate of the scattered polaritons is maximum in an 8-shaped region [Fig. 4(b)]. By contrast, in the high-density regime $\Gamma(\mathbf{k})$ is positive over a large range of k vectors with maxima around $\mathbf{k}_{\text{signal}} \sim 0$ and $\mathbf{k}_{\text{idler}} \sim 2\mathbf{k}_p$ [Fig. 4(c)]. The reason why the shape of the instability regions changes from 8 to pointlike (centered near 0
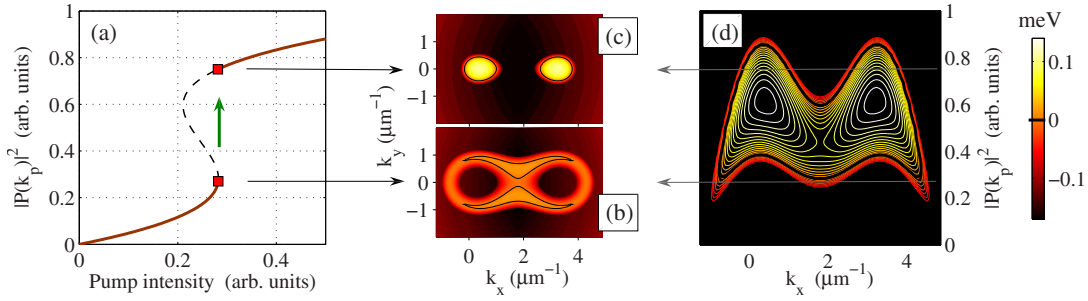
FIG. 4. (Color online) Stability analysis of the solution with a single macroscopically occupied mode (the pumped mode). (a) shows the stationary response function of the pumped LP mode. The solid lines display the "trajectory" that will be experienced by the stable system under the action of a slowly increasing pump. The two points of discontinuity are marked by squares. At these points, the system is expected to have the **k**-space distributions of decay rate $\Gamma(k_x, k_y)$ shown in (b) and (c). (d) represents the distribution of $\Gamma = \Gamma(|\mathcal{P}_0|^2; k_x)|_{k_y=0}$; the contours correspond to the set of values of decay rate from -0.06 to $+0.14$ meV with a step of 0.01 meV. The contours $\Gamma=0$ (stability edges) in (b)–(d) are shown by black lines. Vertical axes in (a) and (d) coincide, and so do the color schemes in (b)–(d) (see the color bar).

and $2\mathbf{k}_p$) when the intracavity polarization of the pumped mode experiences a jump from the lower to the higher S branches can be understood from the distribution $\Gamma = \Gamma(|\mathcal{P}_0|^2; k_x)|_{k_y=0} > 0$ shown in Fig. 4(d). It has a "sleeping-bat" shape, with the top parts of the "wings" above the upper branch of the S curve. Thus, after the jump of the pumped mode polarization $\mathcal{P}(\mathbf{k}_p)$ from the lower to the upper part of the S branch, modes with momenta over a large range of k vectors [$\Delta k \sim 1$ μm^{-1}, see Fig. 4(b)] around $\mathbf{k} \sim 0$ and $\sim 2\mathbf{k}_p$ become strongly unstable. Namely, immediately after the jump of the pump to the upper S branch, many polariton modes acquire a large growth increment of the order of $\Gamma \sim 0.1$ meV, i.e., their population starts to grow with a time constant $\hbar\Gamma^{-1}$ comparable with the MC polariton lifetime.

The predominant scattering pattern in the system is in accord with the distribution of growth increment Γ above the threshold. To describe the experimentally observed transition, we performed numerical solutions of the Gross–Pitaevskii-type equations of Refs. 13–15 in the time domain, which were carried out on a rectangular mesh in momentum space with a step size of 0.1 μm^{-1}, as shown in Figs. 5 and 6. The system parameters are close to the experimentally studied system. The Rabi splitting is 6.4 meV, the exciton-photon detuning is -0.5 meV, the exciton linewidth is 0.2 meV, and the cavity quality factor is $Q \approx 4 \times 10^3$. The steps in the time domain are 20 fs. The time range of the simulated excitation pulse is 1.4 ns. The polariton modes accounted for in the calculation are in the range -4.2 $\mu m^{-1} < k_x < 7.8$ μm^{-1} and -3.0 $\mu m^{-1} < k_y < 3.0$ μm^{-1}, and the calculations show that the population of the boundary modes is negligibly small. The pump wave number is $|\mathbf{k}_p| = k_{px} = 1.8$ μm^{-1} (corresponding to the angle of incidence $\vartheta \approx 14°$) and the pump detuning is $E_p - E_{LP}(\mathbf{k}_p) = 0.48$ meV, which are very close to the experimental parameters in Figs. 2 and 3. As compared to the numerical results presented in Ref. 15, we now increase the number of total polariton modes in the simulation by 2.25 [the mesh step in the (k_x, k_y) momentum space is decreased from 0.15 μm^{-1} in Ref. 15 to 0.10 μm^{-1} in this paper].

Figure 5(a) represents the situation below the threshold: The 8-shaped distribution of intracavity field conforms to the prediction of Refs. 10 and 11 and the experimental results for

intermediate pump intensities [Figs. 3(b) and 3(c)].

Figure 5(b) represents the situation immediately above the threshold: After crossing the critical point on the S-shaped curve of the response in Fig. 4(a), a sharp increase in intracavity field first occurs, accompanied by a fast growing instability of many polariton modes in the range of k vectors where the decay rate $\Gamma(\mathbf{k})$ is positive with maxima around $\mathbf{k} \approx 0$ and $\mathbf{k} \approx 2\mathbf{k}_p$, as shown in Fig. 4(c).
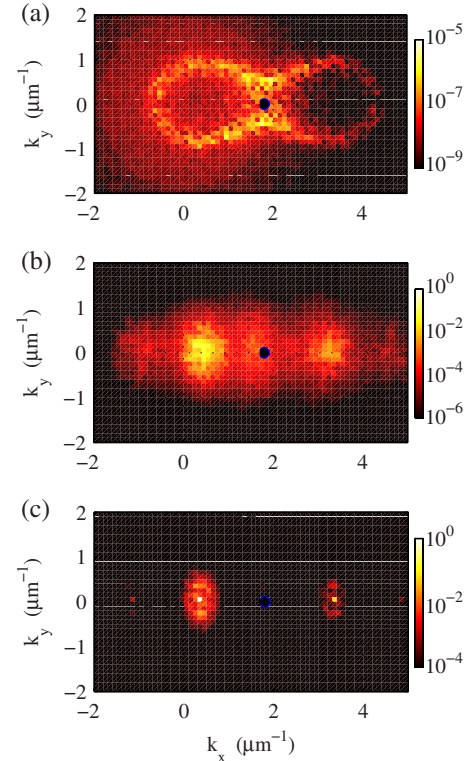

FIG. 5. (Color online) Calculated momentum-space distribution of the intracavity optical field intensity (a) below, (b) in the vicinity, and (c) above the threshold. The calculation is performed with the assumption of a slow increase in pump intensity in the vicinity of the threshold point, $dI/I_{thr}dt \approx 6.4 \times 10^{-5}$ ps^{-1}. Accordingly, (b) displays a transient distribution averaged over 100 ps *after* the drastic breakup of the single-mode solution. At the same time, (c) represents the quasi-steady-state distribution formed $\sim$300 ps later.
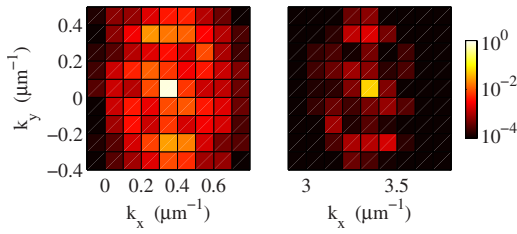
FIG. 6. (Color online) Calculated momentum-space distribution of the intracavity optical field intensity above the threshold of Fig. 5(c) in a magnified scale near $\mathbf{k} \sim 0$ (left panel) and $\mathbf{k} \sim 2\mathbf{k}_p$ (right panel). The rectangular mesh shown, with a step of 0.1 μm^{-1}, corresponds to the discretization of our numerical scheme. It is seen that the final macroscopically occupied signal state in the numerical model is slightly displaced from $\mathbf{k}=0$ to $k_x=0.3$ μm^{-1}. A slight analogous displacement ($k_x \approx 0.15$ μm^{-1}) can also be found in the experimental distribution [see Fig. 3(f)].

Figure 5(c) represents the quasi-steady-state distribution above the threshold. Eventually, in agreement with the experimental observations for high pump intensities in Figs. 3(e) and 3(f), the system evolves to a state with two modes at $\mathbf{k} \approx 0$ and $\mathbf{k} \approx 2\mathbf{k}_p$, with an occupation much greater than all the neighboring ones. The numerical simulation in the time domain[15] shows self-organization: The passage to a quasistationary distribution shown in Fig. 5(b) takes $\tau_{\text{ord}} \sim 3 \times 10^2$ ps after the breakup of the single-mode solution. This time is much greater than the lifetime of a cavity polariton ~ 3 ps. Time-resolved experimental measurements are beyond the scope of this paper and, hence, will be presented elsewhere.

We note that at powers close to the threshold [Fig. 3(d)], we observed polariton emission with k vectors between the maxima of stimulated emission on the 8-shaped figure, as shown in Fig. 3(d) (top panel). The emission pattern occurs along vertical lines parallel to [011] crystallographic axes. We believe that the physical origin of these lines is the result of temporal instabilities of parametric scattering at pump powers close to the threshold of parametric instabilities. In this case, probably most of the time, the population of the pumped mode corresponds to the lower position of the S curve. Thus, scattering occurs in states at k vectors away from $k=0$. This results in pronounced maxima at k vectors in the figure 8. In the real experiment, there is always excess noise, which, for example, may arise from the multimode character of the excitation laser. This increased noise may drive the pumped mode toward the upper branch of the S curve, which leads to temporary amplification of many harmonics with k vectors inside the figure 8, as considered in the paper. Since we record our emission for several seconds in the experiment, the recorded k-space images have both pronounced maxima in the figure 8 and some amplification of polariton harmonics at intermediate k vectors. The direction of the stripes of the polariton emission pattern is very likely related to the asymmetries of the refractive index in the structures, as we have previously reported in real space images.[23]

IV. DISCUSSION AND CONCLUSION

We note that some of us have previously observed the direction of signal emission to be independent of the pump detuning[24] or excitation angle.[25] Also, Baas *et al.*,[19] reported the observation of a signal at 6°. However, the key observation of the abrupt transition between two scattering patterns in the same experimental system has not been previously reported. The observed threshold behavior is analogous to a first-order phase transition in nonlinear systems when the amplitude of a particular amplified mode (order parameter) exhibits a discontinuity as a function of the driving parameter (pump intensity). However, there is a significant difference. In the case of a first-order phase transition, the system exhibits a transition into a different stable state. By contrast, according to numerical simulations, the MC system exhibits a transition into an intermediate state with amplification of many unstable polariton modes, after which further self-organization takes place.

Self-organization occurs due to multiple interactions of a number of amplified polariton modes and, generally speaking, cannot be reduced to a simple breakup of the pumped mode. It may be proven by numerical simulations, which assume only the intermode decays of the pump, i.e., $(\mathbf{k}_p, \mathbf{k}_p) \rightleftarrows (\mathbf{k}, 2\mathbf{k}_p - \mathbf{k})$ and $(\mathbf{k}_p, \mathbf{k}) \rightleftarrows (\mathbf{k}, \mathbf{k}_p)$ for all $\mathbf{k}$ (any "signal-signal" interactions are now excluded). Such a system also exhibits a drastic breakup of the single-mode solution, which is followed by amplification of many modes as considered above. However, in this case the system recovers the figure 8 scattering pattern in the k space after the amplitude of the pumped mode falls due to scattering into numerous signals with various k vectors. Therefore, self-organization of the stimulated polariton-polariton scattering to the macroscopically occupied signal ($\mathbf{k} \sim 0$) and idler states is not observed in numerical simulations if the signal-signal interactions are neglected.

To conclude, we have experimentally demonstrated a sharp transition with an increase in the pump intensity of the scattering pattern of polaritons in a planar MC from an 8-shaped region to a directional one. This transition is theoretically explained via the interplay between the pumped polariton mode bistability and the polariton-polariton parametric scattering instability within a multimode system.

[1] A. V. Kavokin and G. Malpuech, *Cavity Polaritons* (Elsevier, Amsterdam, 2003).

[2] J. P. Karr, A. Baas, R. Houdre, and E. Giacobino, Phys. Rev. A **69**, 031802(R) (2004).

[3] S. Savasta, O. Di Stefano, V. Savona, and W. Langbein, Phys. Rev. Lett. **94**, 246401 (2005).

[4] J. Kasprzak, M. Richard, S. Kundermann, A. Baas, P. Jeambrun, J. M. J. Keeling, F. M. Marchetti, M. H. Szymańska, R. André, J. L. Staehli, V. Savona, P. B. Littlewood, B. Deveaud, and Le Si Dang, Nature (London) **443**, 409 (2006).

[5] D. N. Krizhanovskii, A. P. D. Love, D. Sanvitto, D. M. Whittaker, M. S. Skolnick, and J. S. Roberts, Phys. Rev. B **75**, 233307 (2007).

[6] R. M. Stevenson, V. N. Astratov, M. S. Skolnick, D. M. Whittaker, M. Emam-Ismail, A. I. Tartakovskii, P. G. Savvidis, and J. S. Roberts, Phys. Rev. Lett. **85**, 3680 (2000).

[7] A. I. Tartakovskii, D. N. Krizhanovskii, and V. D. Kulakovskii, Phys. Rev. B **62**, R13298 (2000).

[8] J. J. Baumberg, P. G. Savvidis, R. M. Stevenson, A. I. Tartakovskii, M. S. Skolnick, D. M. Whittaker, and J. S. Roberts, Phys. Rev. B **62**, R16247 (2000).

[9] I. Carusotto and C. Ciuti, Phys. Rev. B **72**, 125335 (2005).

[10] C. Ciuti, P. Schwendimann, and A. Quattropani, Phys. Rev. B **63**, 041303(R) (2001).

[11] W. Langbein, Phys. Rev. B **70**, 205301 (2004).

[12] N. A. Gippius, S. G. Tikhodeev, V. D. Kulakovskii, D. N. Krizhanovskii, and A. I. Tartakovskii, arXiv:cond-mat/0312214 (unpublished).

[13] N. A. Gippius, S. G. Tikhodeev, V. D. Kulakovskii, D. N. Krizhanovskii, and A. I. Tartakovskii, Europhys. Lett. **67**, 997 (2004).

[14] N. A. Gippius and S. G. Tikhodeev, J. Phys.: Condens. Matter **16**, S3653 (2004).

[15] S. S. Gavrilov, N. A. Gippius, V. D. Kulakovskii, and S. G. Tikhodeev, Zh. Eksp. Teor. Fiz. **131**, 819 (2007) [JETP **104**, 715 (2007)].

[16] N. A. Gippius, I. A. Shelykh, D. D. Solnyshkov, S. S. Gavrilov, Y. G. Rubo, A. V. Kavokin, S. G. Tikhodeev, and G. Malpuech, Phys. Rev. Lett. **98**, 236401 (2007).

[17] D. M. Whittaker, Phys. Rev. B **63**, 193305 (2001).

[18] P. G. Savvidis, C. Ciuti, J. J. Baumberg, D. M. Whittaker, M. S. Skolnick, and J. S. Roberts, Phys. Rev. B **64**, 075311 (2001).

[19] A. Baas, J.-Ph. Karr, M. Romanelli, A. Bramati, and E. Giacobino, Phys. Rev. B **70**, 161307(R) (2004).

[20] D. M. Whittaker, Phys. Rev. B **71**, 115301 (2005).

[21] M. Wouters and I. Carusotto, Phys. Rev. B **75**, 075332 (2007).

[22] W. Langbein, Phys. Status Solidi B **242**, 2260 (2005).

[23] D. Sanvitto, D. N. Krizhanovskii, D. M. Whittaker, S. Ceccarelli, M. S. Skolnick, and J. S. Roberts, Phys. Rev. B **73**, 241308(R) (2006).

[24] V. D. Kulakovskii, A. I. Tartakovskii, D. N. Krizhanovskii, N. A. Gippius, M. S. Skolnick, and J. S. Roberts, Nanotechnology **12**, 475 (2001).

[25] R. Butté, M. S. Skolnick, D. M. Whittaker, D. Bajoni, and J. S. Roberts, Phys. Rev. B **68**, 115325 (2003).